EARTH SCIENCES
RESEARCH JOURNAL

Earth Sci. Res. J. Vol. 24, No. 4 (December, 2020): 491-497

UNIVERSIDAD NACIONAL DE COLOMBIA

GPS MEASUREMENTS

High-precision GPS measurement method without geographical restrictions using crowd-sensing technology

Yunxiang Zhang, Bin Wang*, Lei Zhang
College of Information Science & Electronic Technology, Jiamusi University, Jiamusi 154007, China
*Corresponding author: jmsuwang2019@163.com

ABSTRACT

In order to improve the flexibility of GPS measurement, a high-precision GPS measurement method that is not restricted by the geographical location under crowd-sensing technology was proposed. The performance of the crowdsensing network was improved through a regular hexagon-based crowd-smart big data sensing network deployment mechanism. The GPS /SINS/DR fast and high-precision combined measurement methods were used to achieve high-precision measurement without geographical restrictions. It has been verified that the proposed method in this paper has much better stability in the deployment strategy of a regular hexagon than that of the square. The proposed method can achieve fast acquisition of satellite signals and high-precision positioning, and its measurement accuracy in the low-latitude city and high-latitude city is higher than the online measurement method based on Google Earth, indicating that it has significant application value.

Keywords: eCrowd-sensing Technology; Geographical Location, Limitation; High Precision; Global Positioning System; Measurement.

Método de medición GPS de alta precisión sin restricciones geográficas con tecnología de detección de multitudes

RESUMEN

Para mejorar la flexibilidad de la medición GPS se propuso un método de medición GPS de alta precisión que no está restringido por la ubicación geográfica y que se ejecuta bajo tecnología de detección de multitudes. El rendimiento de la red de detección de multitudes se mejoró a través de un mecanismo regular de implementación de redes de detección de macrodatos basado en hexágonos. Se utilizaron los métodos de medición combinados GPS/SINS/DR rápidos para lograr mediciones de alta precisión sin restricciones geográficas. Se ha comprobado que el método propuesto en este trabajo tiene una estabilidad mucho mejor en la estrategia de despliegue del hexágono regular que la del cuadrado. El método propuesto puede lograr una rápida adquisición de señales de satélite y un posicionamiento de alta precisión, y su precisión de medición en ciudades de baja latitud y ciudades de alta latitud es mayor que el método de medición en línea basado en Google Earth, lo que indica que tiene un valor de aplicación significativo.

Palabras clave: bTecnología de detección de multitudes; ubicación geográfica; limitación; alta precisión; Sistema de Posicionamiento Global; medición.

Record
Manuscript received: 03/01/2020
Accepted for publication: 10/08/2020

How to cite item
Zhang, Y., Wang, B., & Zhang, L. (2020). High-Precision Gps Measurement Method Without Geographical Restrictions Using Crowd-Sensing Technology. *Earth Sciences Research Journal*, 24(4), 491-497. DOI: https://doi.org/10.15446/esrj.v24n4.92151

ISSN 1794-6190 e-ISSN 2339-3459

https://doi.org/10.15446/esrj.v24n4.92151

Introduction

Crowdsensing refers to the large-scale and complex society sensing tasks that use the mobile devices (mobile phones, tablets, etc.) of ordinary users as the basic sensing unit, through conscious or unconscious collaboration on mobile Internet, to realize the distribution of sensory tasks and the collection of sensory data as well as complete those complex social sensory tasks. At present, the application scope of crowd-sensing can be divided into three categories: public facilities, environment, and society (Dube et al., 2017).

In terms of public facilities, crowd-sensing can detect traffic congestion, road noise or potholes, search for parking spaces, maintain public facilities such as fire hydrants and traffic lights, and have also been used in monitoring and navigation of real-time traffic (Lowe et al., 2016). For example, through the sensors installed on the car and the GPS, empty parking spaces can be detected and shared on the Internet. Through the CMS system that collects passenger information on the bus, the comfort level of the bus can be evaluated and finally posted on the website. Individuals collect information including pictures and names of bus stations via mobile phones, which helps to predict the arrival time of buses on mobile devices (Chang et al., 2017).

In terms of environment, crowd-sensing technology can be used to collect information such as CO_2 and PM2.5, noise, and water quality in the air. For example, trajectories corresponding to the time and place of mobile users are collected, and known models are used to calculate and collect the content of CO_2 and PM2.5 in the atmosphere. This information is collected through the air quality sensor of the mobile phone to realize the function of environmental monitoring. Because noise is harmful to hearing, a "track-noise" relationship is collected from mobile users to form a noise map and it will be shared on the network. Because people can collect water quality information such as flow, flow velocity, and amount of garbage when passing by rivers, this information collected through mobile apps can be aggregated to a background server and published online (Hoang et al., 2016).

In society, crowdsensing has been applied in social networking, travel, food, and tourism. For example, much social software recommends friends by mutual friends among users. Mobile devices are used to collect user traveling habits and can promote environmentally friendly transportation. Through building a "location-photos" library, people can use the pictures taken to query their geographic information. By personally sharing their food and beverage in the circle of friends, you can not only improve yourself but also give others a good opinion. Based on GPS trajectories and environment information provided by bicycle users, the best cycling route is derived (Zhang et al., 2016).

Although crowdsensing plays a great role in clothing, food, shelter, and transportation, researchers at home and abroad have not stopped studying it in depth. In the past two years, in several well-known academic conferences, many papers have adopted more or less the basic idea of crowd-sensing. The advantage of crowd-sensing is that it has a huge mass base, which makes it outstanding in many fields. In the near future, crowd-sensing will serve society in a smarter and more convenient way (Hsueh & Chen, 2017).

Crowdsensing is a new model that utilizes ubiquitous mobile devices to efficiently collect data and is suitable for many large applications. The entire workflow of crowd-sensing is to use groups to collect data, then analyze and process these data, and finally obtain useful information.

Mi Gensuo et al. adopted GPS/RFID combined location technology and used the CP SO algorithm and BP neural network combined algorithm to filter the output, which achieved high-precision measurement. Foreign researchers proposed using GNSS and map matching algorithms to achieve precise positioning. Liu Jiang et al. use a combination of GPS and inertial measurement units and perform data fusion through the HCX3 robust filtering method. However, the above methods have certain constraints on geographic location. With crowd-sensing technology, the method in this paper realizes a high-precision GPS measurement that is not restricted by geographical location (Cai et al., 2016).

Method

Big data crowd-sensing network deployment mechanism based on a regular hexagon

In this paper, vehicle positioning measurement is taken as an example to study the high-precision GPS measurement method under crowdsensing technology. Crowd-sensing uses the carrying smart devices or wearable devices of people as the basic sensing unit, and wireless communication within a short distance is used to collect and transmit data (Cu et al., 2016). The collection of user participation data is mainly reflected in offline mobile sensing, transmitting data through the human-in-the-loop sensing mode, online social media, and contributing data through various mobile social media. However, due to the limitations of mobile node capabilities and network framework, it is difficult for a crowdsensing network to form a large scale (Li et al., 2019).

Regular hexagonal grid deployment can seamlessly cover the target detection area. Figure 1 shows the details of the regular hexagonal grid deployment mechanism of crowdsensing big data network:

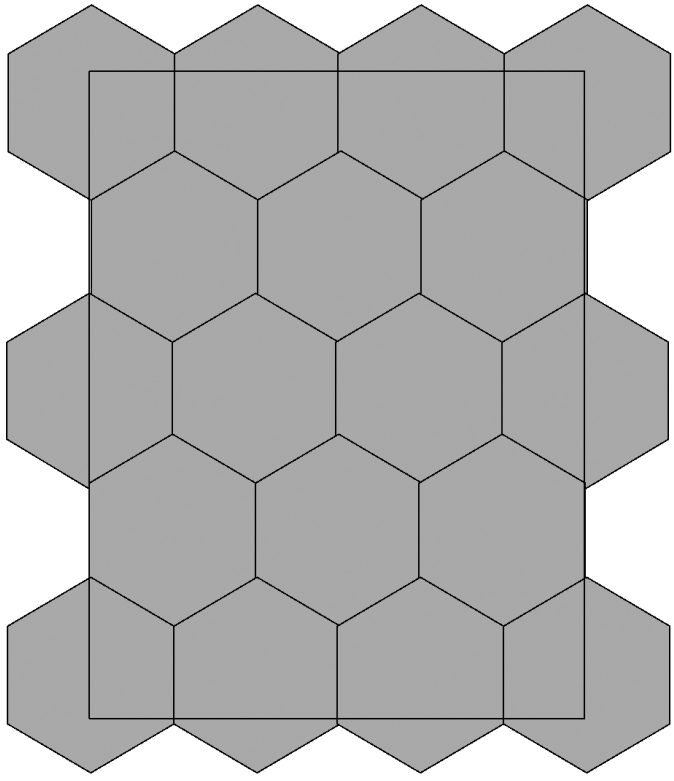

Figure 1. Regular hexagon grid deployment

Supposing that the side length of the regular hexagonal grid is γ, and β is a constant. When the mobile node is located at the positive center of the cluster, the energy consumption of transmitting data between the clusters is:

$$E_{six} = k \times E_{elec} + k \times \varepsilon_{fs} \times d^{\beta} \tag{1}$$

Where k describes the length of the transceiver circuit, ε_{fs} is the parameter under the free space channel model amplifier, E_{elec} the energy consumed to process kbit data. The energy consumption E_{elec} is mainly related to data send distance d.

$$d_{six_{six}} = 2 \times \frac{\sqrt{3}}{2} r_{six}^2 \tag{2}$$

$$r_{six} = \frac{3\sqrt{3}}{2} r_{six}^2 \tag{3}$$

Where r_{six} is the length of the regular hexagon. From formula (2) and formula (3), it can be obtained that:

$$d_{six} = \sqrt{\frac{3\sqrt{3}}{2} \cdot r} \tag{4}$$

The data transmission distance between clusters divided by a regular hexagonal grid is shown in Figure 2.

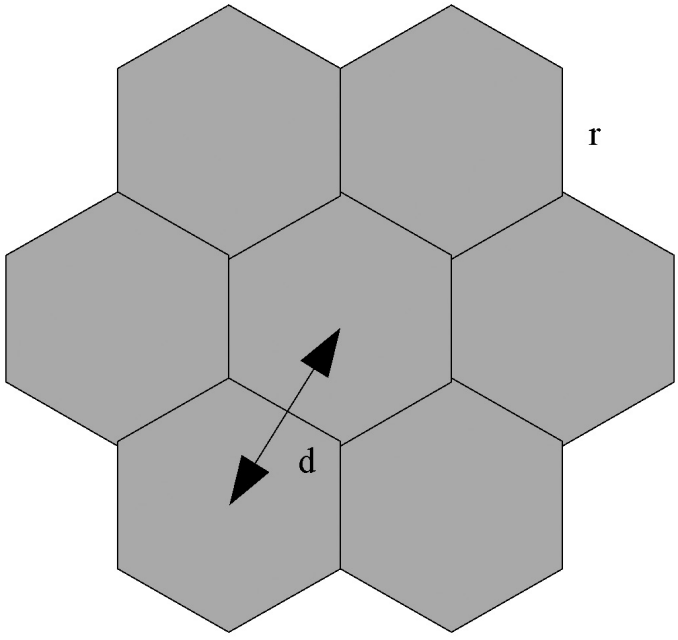

Figure 2. Distance between regular hexagon clusters

In Figure 2, r is a side length of the regular hexagon.

The regular hexagonal division needs to keep the network connected, that is, $d_{six} \le R$. R is the communication radius.

That is: $d_{six} = \sqrt{r^2 + \left(2\sqrt{3}r\right)^2} = \sqrt{13r}$

Equation 3 is brought into the above equation:

$$d_{six} = \sqrt{\frac{26\sqrt{3}}{9} \cdot R_{six}} \tag{5}$$

To keep the network connected, $d_{six} \le R$is essential.

GPS/SINS/DR-based fast and high-precision combined measurement method based on crowd-sensing technology

SINS/DR combined measurement algorithm

The strap-down inertial navigation system (SINS) has been widely used due to its comprehensive navigation information and complete autonomy in providing navigation information, but inertial navigation error will accumulate over time (Kugler, 2017). For vehicle navigation applications, the Dead Reckoning (DR) system is as autonomous as the inertial navigation system, and the DR system error will slowly increase with the accumulation of time. In the case of long-term measurement, the measurement error of SINS is much larger than that of DR (Zhu et al., 2018).

The advantages of the two were used to complement each other, and a SINS/DR combined measurement algorithm was proposed. The algorithm in this paper introduces the strap-down inertial navigation attitude matrix into the dead reckoning state calculation matrix, so the update reckoning matrix can no longer be solved (Golsorkhi et al., 2016). Through this algorithm, the dead reckoning can suppress the divergence of a strap-down inertial navigation error. In this case, the error angle changes of the two are basically the same.

In this method, the quaternion is calculated based on the initial attitude angle, and then the directional cosine matrix C_t^b is obtained. The result is:

$$C_t^b = \begin{bmatrix} \lambda_0^2 + \lambda_1^2 - \lambda_2^2 - \lambda_3^2 & 2\left(\lambda_1\lambda_2 + \lambda_0\lambda_3\right) & 2\left(\lambda_1\lambda_3 - \lambda_0\lambda_2\right) \\ 2\left(\lambda_2\lambda_2 - \lambda_0\lambda_3\right) & \lambda_0^2 + \lambda_1^2 + \lambda_2^2 - \lambda_3^2 & 2\left(\lambda_2\lambda_3 + \lambda_0\lambda_1\right) \\ 2\left(\lambda_2\lambda_3 - \lambda_0\lambda_2\right) & 2\left(\lambda_2\lambda_3 - \lambda_0\lambda_2\right) & \lambda_0^2 - \lambda_1^2 - \lambda_2^2 + \lambda_3^2 \end{bmatrix} \tag{6}$$

Where λ indicates the direction parameter. Relative to the earth coordinate system, the angular velocity of the vehicle geographic coordinate system is:

$$w_{et}^t = \begin{bmatrix} w_{etx}^t \\ w_{ety}^t \\ w_{etz}^t \end{bmatrix} = \begin{bmatrix} -\frac{V_{yt}}{R_{yt}} & \frac{V_{xt}}{R_{xt}} & \frac{V_{yt}}{R_{xt}} \tan L \end{bmatrix} \tag{7}$$

Where V is the vehicle moving acceleration of the coordinate system, R is the crowd-sensing technology communication radius of the coordinate system, L is the vehicle moving distance, the corner mark i is the inertial coordinate system, the corner mark e is the earth coordinate system, the corner mark t is the geographic coordinate system, the corner mark b is the vehicle coordinate system. The specific force information f_{ib}^b obtained by the accelerometer is the specific force of each axis in the carrier coordinate system, but the specific force f_{it}^t required in this paper is the specific force of each axis in the geographic coordinate system. The two specific force can be converted by the following matrix (Liu et al., 2017):

$$f_{it}^t = C_b^t f_{ib}^b \tag{8}$$

According to the proportions, the acceleration in each direction can be calculated. The motion of the vehicle can be regarded as two-dimensional motion in the plane, so only the acceleration in the x and y directions need to be calculated (Coco et al., 2016). Assume that the measured attitude angles are θ and δ, and the odometer trip is S. The equations composed of SINS/DR are:

$$\begin{cases} \dot{V}_{ext}^t = f_{itx}^t - \left(2w_{iez}^t + w_{etz}^t\right)V_{ety}^t - \left(2w_{iez}^t + w_{etz}^t\right)V_{etz}^t \\ \dot{V}_{etx}^t = f_{itx}^t - \left(2w_{iez}^t + w_{etz}^t\right)V_{ety}^t - \left(2w_{iez}^t + w_{etz}^t\right)V_{etz}^t \\ L = L + R\cos\theta \\ \lambda = \lambda + R\cos\gamma \end{cases} \tag{9}$$

The combined measurement results are:

$$\begin{cases} L = \int_0^t \frac{V_{yt}}{R_{yt}} dt + R\cos\theta + L_0 \\ \lambda = \int_0^t \frac{V_{xt}}{R_{xt}} \sec L dt + R\cos\gamma + \lambda_0 \\ \theta = < \arcsin T_{23} \\ \gamma = \arctan\left(-\frac{T_{13}}{T_{33}}\right) \end{cases} \tag{10}$$

Where T describes the time. The above results were used as the update matrix for the second measurement of SINS.

GPS satellite signal acquisition basic principles

In order to track and decode the GPS signal, the GPS signal must be captured first, and the necessary parameters of the captured GPS signal are immediately passed to the tracking process. The navigation message of the satellite can be obtained through the tracking process. Signal acquisition is the process of matching the received satellite signal with the local replica signal. It is achieved by judging whether the carrier frequency and C/A code phase have the maximum correlation with the satellite signal. Before the signal acquisition, the approximate Doppler frequency shift and the initial position of the C/A code phase must be calculated, so the signal acquisition is a two-dimensional search process (Gao et al., 2018).

At present, GPS signal acquisition methods mainly include linear search, parallel code phase search, and parallel frequency search. Parallel code phase search and parallel frequency search are realized by Fourier parallel of one dimensional frequency code or phase code in the two-dimensional search, which can reduce the calculation amount of signal capture and improve the speed of two-dimensional signal search. In this paper, a faster parallel code phase search is used to further improve the acquisition speed (Peyret et al., 2018).

SINS/DR-assisted satellite signal acquisition method

The Doppler frequency shift of a satellite signal is mainly due to the relative motion between the carrier and the satellite, the satellite clock error and the receiver clock error. Its Doppler frequency shift expression is:

$$f_{sh} = f_{dy} + f_{rc} - f_{sc} \tag{11}$$

Where f_{dy} is the Doppler frequency shift between the satellite and the motion carrier, f_{rc} is the clock error frequency of the receiver, f_{sc} is the clock error frequency of the satellite. Among them, the Doppler frequency shift between the satellite and the moving carrier has the most significant influence on f_{sc}.

Ignoring the receiver clock error frequency and the satellite clock error frequency, the Doppler frequency between the satellite and the moving carrier can be predicted by introducing the carrier speed into the satellite navigation messages, which can be expressed as:

$$f_{sh} = f_{wdy} + f_{zdy} \tag{12}$$

Therefore, the parallel code phase search method can be used to introduce SINS/DR combined measurement data into a GPS receiver, and predict the Doppler frequency in advance. It improves the acquisition speed of satellite signals (Gao, 2018).

The implementation process is as follows:

Step 1: The Doppler shift of satellite motion is calculated from the ephemeris:

$$f_{dr} = \frac{f_r v_s r_e}{c r_s} \tag{13}$$

Where f_r is the carrier frequency of the GPS satellite, v_s is the operating speed of the satellite in orbit, r_e is the radius of the earth, c is the speed of light, r_s and is the average radius of the satellite orbit.

Step 2: Calculate the Doppler frequency shift of the carrier motion. From the above SINS/D R combined measurement analysis, the velocity of the motion carrier can be expressed as:

$$v_z = \sqrt{\left(V_{ets}^t\right)^2 + \left(V_{ety}^t\right)^2} \tag{14}$$

The Doppler frequency shift of the motion carrier is:

$$f_z = \frac{f_r \sqrt{\left(V_{ets}^t\right)^2 \left(V_{ety}^t\right)^2}}{c} \tag{15}$$

Step 3: The Doppler frequency shift can be obtained through the above calculation:

$$f_{sh} = \frac{f_r}{c}\left(\frac{v_s r_e}{r_s} + \sqrt{\left(V_{etx}^t\right)^2 + \left(V_{etx}^t\right)^2}\right) \tag{16}$$

Step 4: The satellite signal was mixed with the local replica signal (with Doppler frequency shift assistance) to obtain I and Q signals (Hoang et al., 2016).

Step 5: Fourier transform was performed on the I and Q signals. Then they were multiplied with the local C/A code that completed the complex conjugate transform and Fourier transform. And modulus operation was performed on the result, obtaining the last captured result (Li & Xu, 2016).

Data fusion processing algorithm

When the vehicle is running at high speed, its high dynamics and complicated external environment will seriously interfere with the normal measurement work of the GPS receiver. Therefore, when improving the satellite signal acquisition capability, ensuring the SINS/DR data connection if the satellite measurement data is interrupted is the key to improving measurement accuracy. This paper combines the least square method with the Kalman filter algorithm to propose a new data fusion processing algorithm, LSKF.

The core idea of LSKF is to determine whether the satellite measurement data is lost through the acquisition of satellite signals. In the case of data loss, the least square method is used to estimate the satellite measurement data, and the results are used as quasi observations and will be further processed by Kalman filter. When the data is complete, Kalman filter is directly used. This method avoids the non-linear errors in the observation equation and achieves high-precision tracking measurement of the moving vehicle.

Analysis of LSKF algorithm model

The least squares estimate is obtained from the navigation measurement data. It is assumed that the measurement data (x_u, y_u) before GPS satellite information loss can be measured, and u represents a constant. The route distance is regarded as an infinitely small value. For infinitely small distances, the route can be regarded as a straight line. With the least-square method, the fitting curve can be expressed as:

$$y_n = a + bx_u \tag{17}$$

Where a and b describe vectors.

Supposing that:

$$J(a,b) = \sum_{u=1}^{n}\left[y_u - \left(a + bx_u\right)\right]^2 \tag{18}$$

Where n = 1,2,3 ..., n. The result is:

$$\begin{cases} nb + b\sum_{u=1}^{n} x_u = \sum_{u=1}^{n} y_u \\ a\sum_{u=1}^{n} x_u + b\sum_{u=1}^{n} x_u^2 = \sum_{u=1}^{n} x_u y_u \end{cases} \tag{19}$$

The least squares solution can be obtained through equations (17) to (19). In order to realize the simulation calculation, the matrix is expressed as:

$$\begin{bmatrix} a \\ b \end{bmatrix} = \begin{bmatrix} 1 & x_1 \\ \vdots & \vdots \\ 1 & x_u \end{bmatrix}^T \begin{bmatrix} 1 & x_1 \\ \vdots & \vdots \\ 1 & x_u \end{bmatrix}^{-1} \begin{bmatrix} 1 & x_1 \\ \vdots & \vdots \\ 1 & \boldsymbol{x}_u \end{bmatrix}^T \begin{bmatrix} Y_1 \\ \vdots \\ y_u \end{bmatrix} \tag{20}$$

The results obtained previously were used as quasi observations and a Kalman filter calculation model was introduced. Kalman filter is a recursive linear minimum variance estimation technique that uses recursive estimation to calculate continuous measurement data. The GPS measurement data was processed by the least square method, and the obtained coordinates were used as quasi observations. Because the processed data was approximately linear, Kalman filter was used to optimize the measurement results (Li et al., 2016). The Kalman filter steps are as follows:

(1) The initial values are calculated. When u =1 and u = 2, the train positions calculated by the least squares method are (x_1, y_1) and (x_2, y_2). And the system initial value X_2 can be expressed as:

$$X_2 = \begin{bmatrix} x_2 & y_2 & x_2 - x_1 & y_2 & y_1 \end{bmatrix}^T \tag{21}$$

(2) Using the initial value and state variable in step 1, the estimated value of the system when $u \geq 3$ is:

$$\begin{cases} x(k,k-1) = y(k,k-1)x(k-1) \\ P(k,k-1) = y(k,k-1)P(k-1)y^* + Q(k-1) \end{cases} \tag{22}$$

Where K represents the state variable, P represents the observed value, Q represents the estimated value.

(3) The error of the observed value to the estimated value is corrected as:

$$\begin{cases} P(k)=\left\{\left[P(k,k-1)\right]^{-1}+P^{T}R^{-1}(k-1)P\right\}^{-1} \\ x(k)=x(k,k-1)+P(k)\left[z(k)-Px(k,k-1)\right] \\ P(k)=P(k)P^{T}R^{-1}(k-1) \end{cases} \quad (23)$$

Result

Network connectivity

In order to verify the advantages of the deployment strategy proposed by this method, Matlab2016a was used to analyze the connectivity stability of the crowd-sensing network. The square grid division was compared with the regular hexagonal grid division in this paper, as shown in Figure 3.

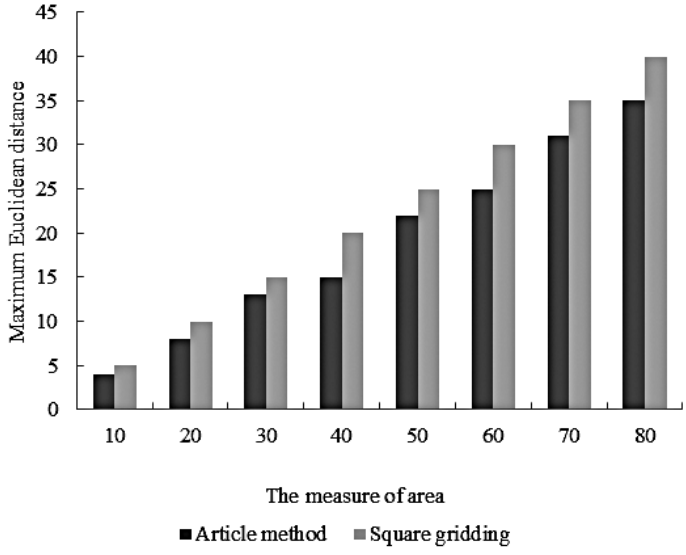

Figure 3. Maximum Euclidean distance

It can be seen from Figure 3 that the maximum Euclidean distance gradually increases with the increase of the area. The maximum Euclidean distance of the square grid division is significantly higher than that of the regular hexagonal grid division. The quality gradually becomes unstable with the increase of the maximum Euclidean distance. Because regular hexagonal grid division has smaller maximum Euclidean distance, and its communication quality is slightly better than that of square grid division, indicating the deployment strategy of the method in this paper has advantages.

GPS satellite signal acquisition verification

According to the "Specifications for the Design of High-speed Railways", railways designed for passenger trains with a travel speed of 250 to 350 km/h are called high-speed railways. Therefore, in this paper, a high-speed motion carrier is used to simulate the rapid driving of the vehicle, and the debugging simulation is carried out on computer. The Doppler frequency shift of the signal carrier was set as ± 5 kHz and the maximum travel speed of the carrier was set as 300km/h. Satellite signal acquisition simulation analysis was performed on the traditional GPS receiver and the GPS receiver with carrier motion Doppler frequency shift. The peak values of the signals captured by the two receivers are shown in Figure 4.

Obviously, after Doppler frequency shift is introduced in this method, the correlation of acquisition has been greatly improved, and the peak value has been improved.

Fig. 5 is the time curve of capturing 20 signals with different intensities in both cases. Without the introduction of carrier motion Doppler frequency shift, the GPS satellite signal acquisition time is shown in Figure 5.

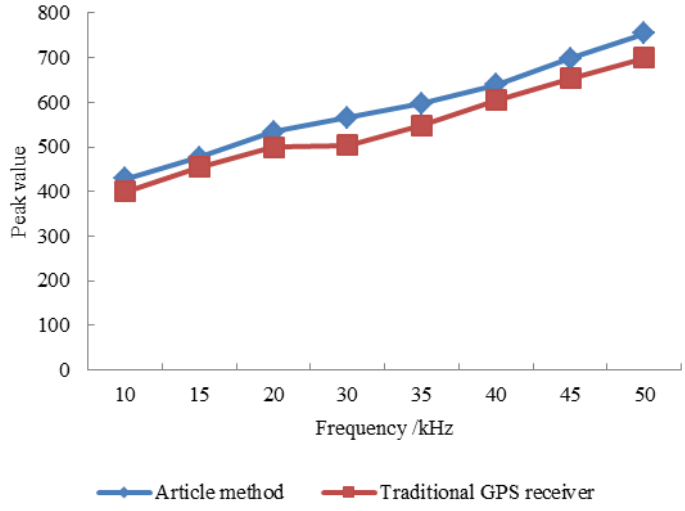

Figure 4. Verification results of GPS satellite signal acquisition

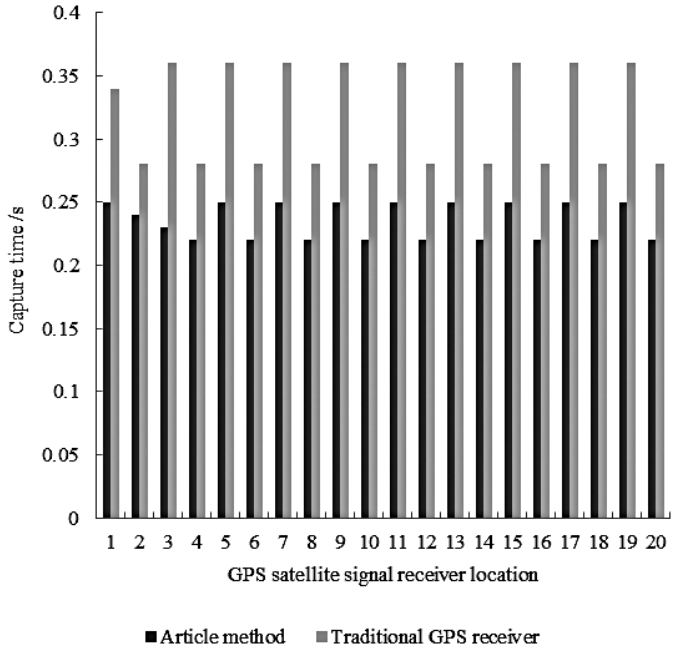

Figure 5. GPS satellite signal acquisition time

In Figure 5, the maximum value of the acquisition time for a conventional GPS receiver is 0.36s. In the case of the method in this paper, the maximum value of the acquisition time is about 0.25s. The capture speed was improved by 0.11s.

Suppose that 10 test positions are the coordinate positions of 10 points evenly distributed on a road. The total length of the test road is 1.5 km. Positions 2, 6, and 10 are on the road section without signal blocking. Signals in positions 1, 3, 4, 5, 7, 8, and 9 are blocked by trees and houses to varying degrees, and the other test environments are exactly the same. Fig. 6 shows the data of satellite capture measurement data using the traditional GPS receiver and the GPS receiver proposed in this paper:

As can be seen in Fig. 6, after using a GPS receiver that introduces Doppler frequency shift of the motion carrier, and the method in this paper successfully captures measurements more often than an ordinary GPS receiver.

Measurement accuracy

In order to further verify the measurement accuracy of the method in this paper. The method in this paper was applied to vehicle measurement in high

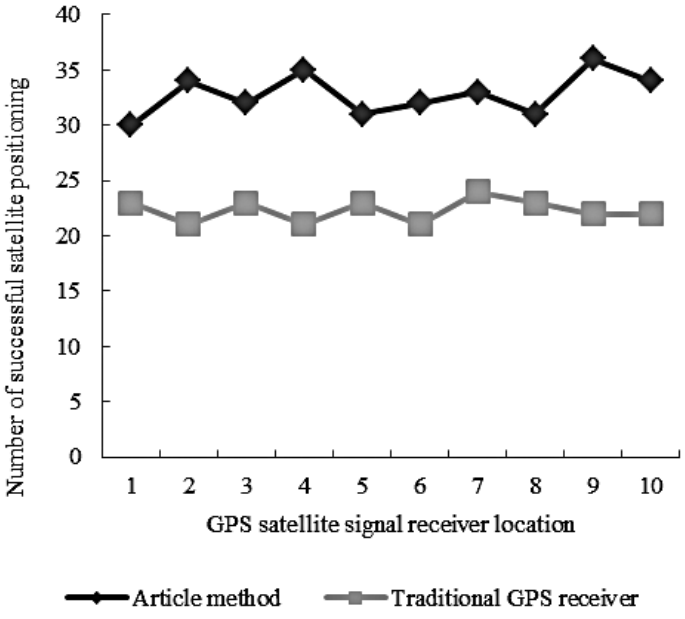

Figure 6. GPS Comparison of satellite acquisition and positioning

latitude city London and low latitude city Lhasa. The geographic location online measurement method based on Google Earth was used to make a comparison. The results are shown in Figure 7 and Figure 8.

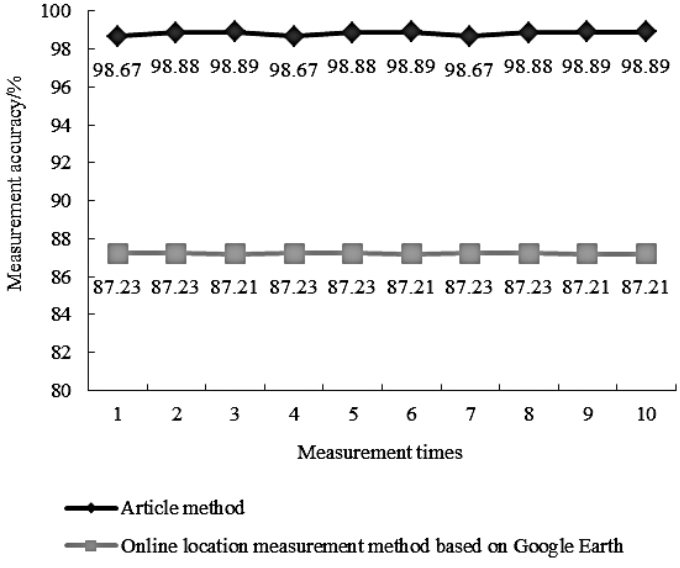

Figure 7. Measurement accuracy test results of two methods in high latitude City

It can be seen from Fig. 7 and Fig. 8 that the accuracy of the method in this paper is as high as 98.89% and 98.99% in the measurement of vehicles in low-latitude city and high-latitude city, respectively. Compared with the online measurement method based on Google Earth, this method has higher precision.

Discussion

As an emerging research field, a crowd-sensing network is facing many challenges, which can be summarized as the following seven aspects.

(1) The common platform of a crowd-sensing network. At present, academia and industry have designed and developed a variety of crowd-sensing applications. They usually have similar or partially overlapping functions and require the same or interrelated sensing data. They are facing a series of

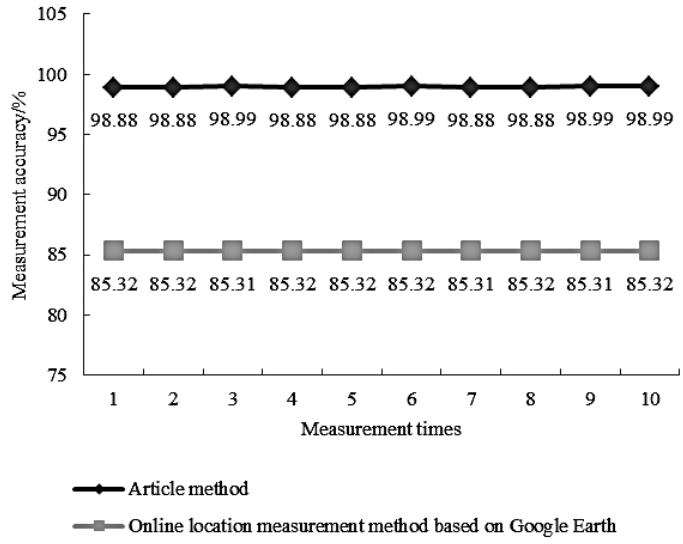

Figure 8. Measurement accuracy test results of two methods in low latitude City

common issues and challenges such as data collection, resource allocation, energy conservation, user motivation, security and privacy. At present, this independent development model is very inefficient, resulting in a great waste of resources. Therefore, building a common platform for the crowd-sensing network is a basic problem that should be solved urgently in this field.

(2) Front-end processing of crowd-sensing data. The raw sensing data collected by sensors such as GPS, accelerometer, microphone, and camera are usually very noisy, incomplete or redundant, and it is difficult to use them directly. Therefore, effective front-end processing algorithms need to be designed, mainly including two types. One is data quality enhancement, including operations such as eliminating noise, filtering abnormal data, recovering lost data, repairing and enhancing low-quality images. The other is context inference, which includes inferring traffic patterns, sports patterns, and social occasions (such as meetings, calls, watching TV, etc.) of users and the surrounding environment (such as road bumps, noise levels, etc.).

(3) Efficient transmission of crowd-sensing data. Many crowd-sensing applications need to continuously collect the sensing data and transmit it to the data center. The transmission method based on the mobile cellular network will consume equipment power and data traffic of the users, and put a lot of pressure on the mobile cellular network. Therefore, energy-efficient data transmission methods need to be designed. For example, in the short-range wireless communication methods, the opportunity of users to contact each other or users to contact with WiFi hotspots is used to forward data.

(4) Value mining of crowd-sensing data. Crowd-sensing data comes from different users, different sensors, and has features such as multi-modality and multi-association. These massive data must be intelligently analyzed and mined to effectively exert value and form a leap from data to information and even to knowledge. The technologies involved include big data storage and processing, data quality management, and multi-modal data mining.

(5) Resource optimization of crowd-sensing network. Overcoming the resource constraints of mobile nodes in the terms of energy, bandwidth, and computing is the key to the practical application of the crowd-sensing network. First, the number of users and the availability of sensors change dynamically over time, and it is difficult to build models and make predictions accurately based on energy and bandwidth requirements to complete specific sensing tasks. Second, it is necessary to select an effective subset from a large number of users with different sensing capabilities, and reasonably schedule the sensing and communication resources under resource constraints.

(6) Incentive mechanism of crowd-sensing network. Crowd-sensing applications rely on the participation of a large number of ordinary users, and the users will consume their device power, computing, storage, communication and other resources and bear the threat of privacy leakage when participating. Therefore, a reasonable incentive mechanism must be designed as repay for the users, which ensures the quality of required data.

(7) Security and privacy protection of the crowd-sensing network. Sensing data may leak the privacy and sensitive information of the users, so a reasonable privacy protection mechanism must be designed to ensure the privacy of the users while completing data collection as much as possible.

Conclusion

Crowd-sensing has risen in recent years and is still in its early stages. Its development depends largely on the development and popularity of mobile devices. In the process of crowd-sensing, the collection and use of data is very important.

Based on crowd-sensing technology, this paper proposes a high-precision GPS measurement method that is not restricted by geographical location. A crowd-sensing big data network deployment mechanism based on regular hexagon was designed. Based on this mechanism, a rapid high-precision GPS/SINS/DR combined method was used to achieve high-precision measurement without geographical restrictions. The crowd-sensing network in this paper has high network connectivity and good communication quality. And after Doppler frequency shift is introduced into this method, the correlation of its acquisition has been greatly improved, and the acquisition peak has been improved. The traditional GPS receiver has a maximum acquisition time of 0.36s without the carrier motion Doppler frequency shift. In this method, the carrier motion Doppler frequency shift is used, and the maximum acquisition time is about 0.25s, which is increased by 0.11s. And the number of acquisition measurements is higher than traditional GPS receivers. In low-latitude city and high-latitude city, the measurement accuracy of the method in this paper is as high as 98.89% and 98.99%, which illustrates that it can achieve high-precision GPS measurement without geographical restrictions.

In the location service application, the crowd-sensing network system should pay attention to the setting of location privacy protection and incentive mechanism. Location privacy leakage is the biggest threat to such applications. In location-based services, sensitive data is primarily user location information. An attacker can infer the sensitive information of the users based on the location information sent by them, including home address, commuting route, etc. In a crowd-sensing system based on location service, each user sends data to the server. This data often contains information about user privacy, such as their location and time. In the crowd-sensing system, any individual or organization can initiate tasks and motivate users to participate in sending data, so the application server is considered untrusted. If location information of the users is leaked to an untrusted server, it will cause great harm to the user. Even if the user does not send data using their real name, the server can identify the specific user or reduce the anonymity of the user according to the relevance of the data sent by the user. The goal of user location privacy protection is that the server cannot establish the association between user identity and data, so the server cannot identify a specific user based on the data sent by the user. How to protect the location privacy of the users is a major problem faced by the crowd-sensing system.

Reference

Cai, A. H., He, J. W., & Wang, P. (2016). Experiment and Error Analysis of Path Planning for Sonobuoy Array Deployment. *Journal of China Academy of Electronics and Information Technology*, 11, 21-24.

Chang, H. K., Sun, Y. K., & Chan, G. P. (2017). An Adaptive Complex-EKF-Based DOA Estimation for GPS Spoofing Detection. *I*ET *Signal Processing*, 12, 174-181.

Coco, D. S., Gaussiran, T. L., & Coker, C. (2016). Passive detection of sporadic E using GPS phase measurements. *Radio Science*, 30, 1869-1874.

Dube, P., Bernard, J. E., & Gertsvolf, M. (2017). Absolute frequency measurement of the $^{88}Sr^{+}$ clock transition using a GPS link to the SI second. *Metrologia*, 54, 290-298.

Gao, L. (2018). Urban Strip Road Landscape Sharp Feature Extraction Integrity Optimization Simulation. *Computer Simulation*, 7, 261-264.

Gao, R. M., Yang, W. J., & Dai, Q. (2018). Characteristic Polynomials of Graphical Arrangements Corresponding to Wheel Graphs and Join Graphs. *Journal of Jilin University (Science Edition),* 56, 859-863.

Golsorkhi, M. S., Lu, D., & Guerrero, J. M. (2016). A GPS-based decentralized control method for islanded microgrids. *IEEE Transactions on Power Electronics*, 32(2):1-1.

Gu, Y., Yuan, L., Fan, D., You, W., & Su, Y. (2016). Seasonal crustal vertical deformation induced by environmental mass loading in mainland China derived from GPS, GRACE and surface loading models. *Advances in Space Research*, 59, 88-102.

Hoang, G. M., Denis, B., Harri, J., & Slock, D. T. M. (2016). Breaking the gridlock of spatial correlations in GPS-aided IEEE 802.11p-based cooperative positioning. *IEEE Transactions on Vehicular Technology*, 65, 9554-9569.

Hsueh Y. L., & Chen, H. C. (2017). Map Matching for Low-Sampling-Rate GPS Trajectories by Exploring Real-time Moving Directions. *Information Sciences*, 434, 55-69.

Kugler, L. (2017). Why GPS spoofing is a threat to companies, countries. *Communications of the Acm*, 60, 18-19.

Li, X., & Xu, Q. (2016). A Reliable Fusion Positioning Strategy for Land Vehicles in GPS-Denied Environments Based on Low-Cost Sensors. *IEEE Transactions on Industrial Electronics*, 99, 1-1.

Li, H., Guo, Z. Y., Liu, C., & Zhao, Y. (2019). Stability Improvement Method for Cascaded DC-DC Converters with Additional Inductor Current Linear Feedback Control. *Journal of Power Supply*, 17, 103-110.

Li, Z., Filev, D. P., Kolmanovsky, I., Atkins, E., & Lu, J. (2016). A New Clustering Algorithm for Processing GPS-Based Road Anomaly Reports With a Mahalanobis Distance. *IEEE Transactions on Intelligent Transportation Systems*, 99, 1-9.

Liu, X. L., Chang, J. C., & Liu, R. N. (2107). Synthesis method of initial noise samples of oil pump cavitation fault based on characteristic frequency analysis. *Automation & Instrumentation*, 12, 62-164.

Lowe, S. T., LaBrecque, J. L., Zuffada, C., Romans, L. J., Young, L. E., & Hajj, G. A. (2016). First spaceborne observation of an Earth-reflected GPS signal. *Radio Science*, 37, 7-1-7-28.

Peyret, M., Djamour, Y., Hessami, K., Regard, V., Bellier, O., Vernant, P., Daignieres, M., Nankali, H., Van Gorp, S., Goudarzi, M., Chery, J., Bayer, R., & Rigoulay, M. (2018). Present-day strain distribution across the Minab-Zendan-Palami fault system from dense GPS transects. *Geophysical Journal International*, 179, 751-762.

Zhang, D. H., Xiao, Z., Igarashi, K., & Ma, G. Y. (2016). GPS-derived ionospheric total electron content response to a solar flare that occurred on 14 July 2000. *Radio Science*, 37, 19-1-19-11.

Zhu, Z. G., He, B. B., & Xue, R. (2018). Image feature recognition method for dangerous situation in intelligent substation. *Chinese Journal of Power Sources*, 42, 597-600.